Mater. Res. Soc. Symp. Proc. Vol. 1148 © 2009 Materials Research Society 1148-PP12-02

Fabrication and Characterization of Electrically Functional Lanthanum Hexaboride Thin Films on Ultrasmooth Sapphire Substrates

Yushi Kato[1], Yusaburo Ono[1], Yasuyuki Akita[1], Makoto Hosaka[1], Naoki Shiraishi[1], Nobuo Tsuchimine[2], Susumu Kobayashi[2], and Mamoru Yoshimoto[1]
[1]Department of Innovative & Engineered Materials, Tokyo Institute of Technology, Yokohama 226-8503, Japan.
[2]TOSHIMA Manufacturing Company Limited, Saitama 355-0036, Japan.

ABSTRACT

The crystal growth of lanthanum hexaboride (LaB_6) thin films was examined by applying the laser molecular beam epitaxy (laser MBE) process. C-axis (100) highly-oriented LaB_6 thin films could be fabricated on ultrasmooth sapphire (α-Al_2O_3 single crystal) (0001) substrates with atomic steps of 0.2 nm in height and atomically flat terraces. The obtained film exhibited a smooth surface with root mean square roughness of 0.15 nm. The lattice parameter of the LaB_6 thin film was close to the bulk value reported previously. In the case of deposition on commercial mirror-polished sapphire substrates, the grown film was amorphous. The resistivity of the prepared crystalline LaB_6 thin films was as low as 2.2×10^{-4} Ω cm and almost constant in the temperature range of 10–300 K.

INTRODUCTION

Lanthanum hexaboride (LaB_6) is characterized by a high melting temperature, excellent thermal stability, high hardness, and excellent chemical stability [1–9]. It has already been applied to practical use in thermionic electron sources for TEM, SEM, and flat panel displays, which can offer high brightness and long service life because of the compound's extremely small work function (~2.4 eV), high current and voltage capability, and low vapor pressure at high temperature. The crystal structure of LaB_6 is a simple cubic CsCl-type arrangement of B_6-octahedra and metal ions [1–5], and the electric conduction of LaB_6 shows metallic properties [7]. In addition, the electrical properties of hexaborides including various metal ions show a wide variation from semiconductor to superconductor [10], by doping divalent or trivalent ions into the crystal structure [11, 12].

The investigations providing the results outlined above have mostly been conducted on bulk samples of LaB_6 [1–9]; in contrast, the properties of LaB_6 thin films have not been well explored. There have been reported a few attempts to prepare LaB_6 nanowire by chemical vapor deposition (CVD) [13], and LaB_6 thin films by sputtering [14, 15], e-beam evaporation [16], and pulsed laser deposition (PLD) [17–19]. However, there are no reports on fabrication of epitaxial LaB_6 thin films. We have previously investigated low temperature epitaxial growth of functional ceramic thin films of oxides [20–22] and nitrides [23, 24] by laser MBE (i.e., pulsed laser deposition in ultra-high-vacuum) using ultrasmooth sapphire (α-Al_2O_3 single crystal) (0001) substrates. These smooth substrates have atomic steps of 0.2 nm in height and atomically flat terraces of 60–80 nm in width [25]. Laser MBE has been intensively applied to the growth of

epitaxial thin films of high-melting-point ceramics at relatively low substrate temperatures. In this paper, we examined the growth of LaB_6 thin films by laser MBE and characterized their morphologic, crystallographic, and electrical properties.

EXPERIMENT

Fabrication of LaB_6 thin films was carried out using laser MBE (base pressure of ~10^{-7} Pa) on ultrasmooth sapphire (0001) substrates as well as commercial mirror-polished sapphire (0001) substrates. A pulsed KrF excimer laser of wavelength λ = 248 nm and pulse duration s = 20 ns was focused on a sintered ceramic target of LaB_6 (99.5% purity) with energy density of 3.0 J/cm^2 and frequency of 5 Hz. The distance between the substrate and the target was 5 cm. The ablated particles collide with the sapphire (0001) substrates heated at 800°C to form the film. The ultrasmooth sapphire substrate was obtained by annealing the commercial mirror-polished α-Al_2O_3 single crystal wafer at 1000°C for 3 h in air [25]. The crystallographic characterization was carried out by *ex-situ* X-ray diffraction (MXP-M18, Bruker AXS) using a CuKα-characteristic X-ray (λ = 0.1542 nm). The surface morphologies of the film were observed in air by atomic force microscopy (AFM) (SPI-3700, Seiko Instruments). The resistivity of the obtained film was measured by the conventional four-probe method in a temperature range of 10–300 K.

RESULTS AND DISCUSSION

Figure 1 shows the AFM surface image of the commercial mirror-polished sapphire (0001) substrate (a), the AFM surface image of the ultrasmooth sapphire (0001) substrate (b), and the cross-sectional profile (c) of Figure 1 (b). The step height is uniformly about 0.2 nm, and the terrace width is 60–80 nm, as shown in Figure 1 (c).

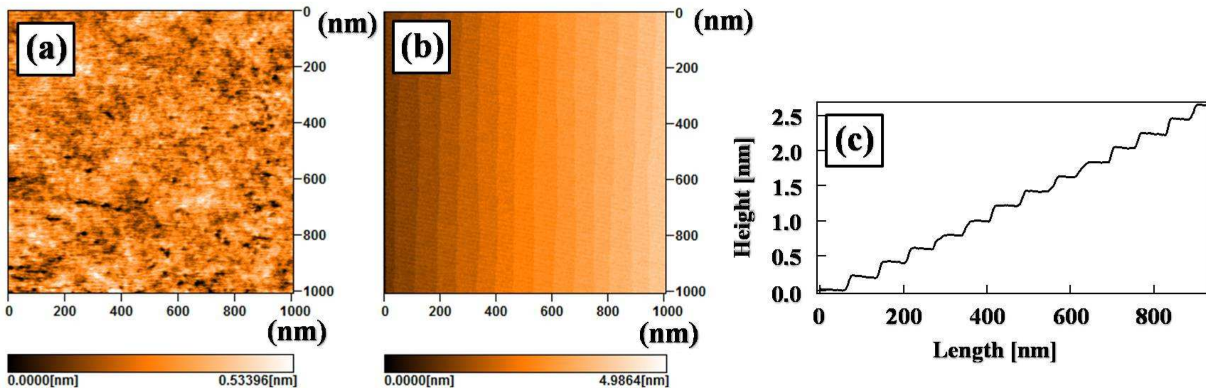

Figure 1. The AFM surface image of the commercial mirror-polished sapphire (0001) substrate (a), the AFM surface image of the ultrasmooth sapphire (0001) substrate (b), and the cross-sectional profile (c) of Figure 1 (b).

Figure 2 shows AFM surface images of the LaB_6 thin films deposited on the commercial mirror-polished sapphire substrate (a) and the ultrasmooth sapphire substrate (b). Compared with the films grown on the commercial mirror-polished substrate, nanocrystals on the ultrasmooth

substrate seem to be grown along the atomic steps on the substrate. This anisotropic crystallization may be enhanced by preferential trapping of film precursors at the kinks of the step edge as well as migration of the adsorbed atoms along the atomic steps on the terrace surface. As a result, nanocrystal grains are considered to be nucleated and grown along the atomic steps, as shown in Figure 2 (b). In addition, root mean square (RMS) roughness of the prepared thin film on the commercial and ultrasmooth sapphire substrate was 0.20 nm and 0.15 nm, respectively. The surface of the prepared thin film on the ultrasmooth sapphire substrate was smoother than that of the film on the commercial mirror-polished substrate, reflecting the surface morphology of the used substrate.

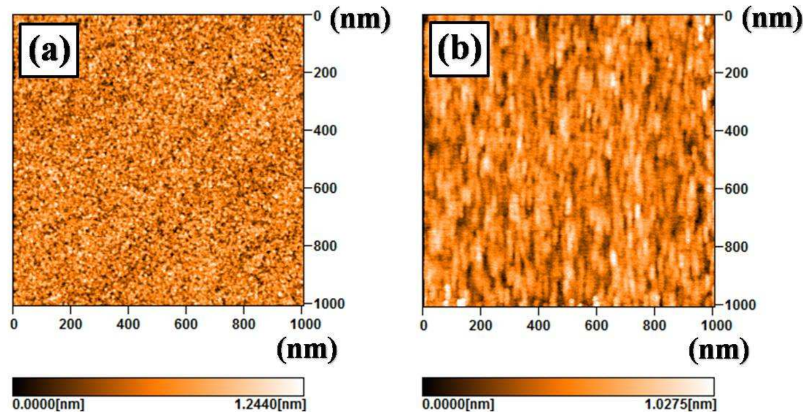

Figure 2. AFM surface images of the prepared LaB_6 thin films on the commercial mirror-polished sapphire substrate (a) and the ultrasmooth sapphire substrate (b).

Figure 3 shows the XRD patterns of the LaB_6 thin films deposited on the commercial mirror-polished sapphire substrate (a) and the ultrasmooth sapphire substrate (b). C-axis (100) highly-oriented crystalline LaB_6 thin films could be fabricated on the ultrasmooth sapphire substrate as shown in Figure 3 (b). In contrast, the crystalline thin film could not be prepared on the commercial mirror-polished sapphire substrate, indicating that the film deposited on the mirror-polished substrate is amorphous. The lattice parameter a_0 of the prepared (100) highly-oriented LaB_6 thin films was 0.4159 nm, which is close to the lattice parameter ($a_0 = 0.4157$ nm) of bulk LaB_6 in the JCPDS data base. This suggests that the obtained (100) highly-oriented LaB_6 thin films have a stoichiometric composition similar to that of the bulk LaB_6.

The above results on AFM and XRD analyses show that the atomic scale surface morphology of the substrate greatly affects the crystal growth behavior of boride thin films. Figure 4 presents the schematic diagram of LaB_6 crystal growth on the ultrasmooth sapphire substrate. It shows the effect of atomic steps and atomically flat terraces on the nucleation and growth of the film. During the deposition, adsorbed film precursors of atoms, ions and clusters migrate on the flat terrace, and then are preferentially trapped near the atomic steps, where a number of active and unstable dangling bonds exist more densely than on the atomically flat terraces. As a result, the growth behavior of LaB_6 nanocrystals has a possibility of in-plane crystal alignment or anisotropic crystallization concerning with the atomic steps. On the other hand, as the films tend to grow with a surface energy as low as possible, the (100) highly-oriented growth of the LaB_6 thin films in this study well reflects the order of estimated surface energy for each plane, such as (100) < (110) < (111) plane [14, 15].

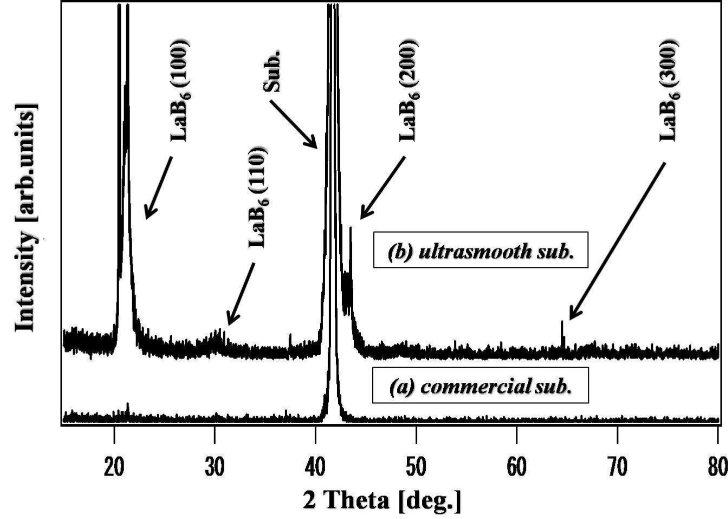

Figure 3. XRD patterns of the LaB_6 thin films deposited on the commercial mirror-polished sapphire substrate (a) and the ultrasmooth sapphire substrate (b).

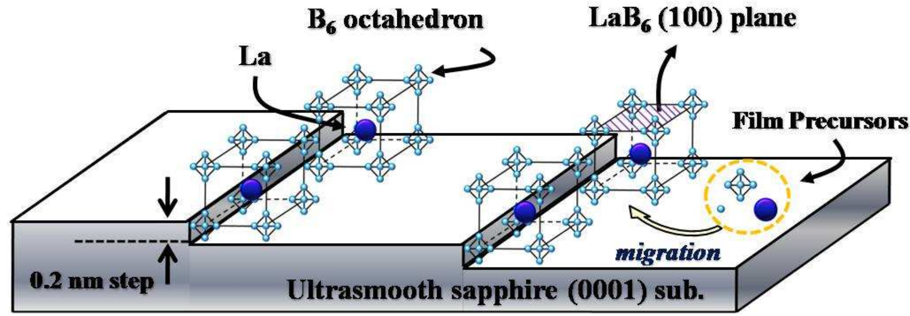

Figure 4. The schematic diagram of LaB_6 crystal growth on the ultrasmooth sapphire substrate.

Figure 5 indicates the resistivity–temperature curve of the LaB_6 thin film prepared on the ultrasmooth sapphire substrate. The electrical property of the prepared (100) highly-oriented LaB_6 thin films shows a metallic behavior, and the resistivity is almost constant (2.2×10^{-4} Ω cm) in the temperature range of 10–300 K. In contrast, the resistivity of the amorphous LaB_6 thin films grown on the mirror-polished sapphire substrate was about 6.0×10^{-4} Ω cm at room temperature. The room-temperature resistivity of the (100) highly-oriented LaB_6 thin films is about 20 times larger than that of the single crystalline LaB_6 as reported previously. In general, the difference of the resistivity between bulk and thin film is considered to be caused by the effect of impurity, deficiency, internal stress, and compositional unstoichiometry that exist in the thin film system. Considering the lattice parameter close to that of the bulk, impurities such as oxygen or other metal ions, or crystallographic deficiency seems to increase the resistivity of the film. The mean free path *l* of an electron carrier in our sample can be estimated using Matthiessen's rule as follows [16]:

$$l = (r.r.r. - 1)[\rho l]_{Bulk} / \rho(T = 300K), \quad (1)$$

where $[\rho l]_{Bulk}$ is the bulk value of ρl (2.1×10^{-11} Ω cm^2 for LaB_6 [7]), *r.r.r.* is the residual resistance ratio, and $\rho(T = 300\ K)$ is the bulk resistivity at 300 K (8.9×10^{-6} Ω cm for LaB_6), respectively. Thus, the mean free path l of the film is about 1.1 nm, i.e., much smaller than that of the bulk material (~6.98 μm [7, 16]). The grain size of the LaB_6 thin film is estimated to be about 25 nm from calculation using Sherrer's equation in XRD peaks. This value corresponds well with the grain size in the AFM image as shown in Figure 2 (b). As the grain size d is larger than the mean free path l estimated for this sample, the effect of grain-boundary scattering on electron conduction is considered to be smaller than that of inter-grain scattering including electron–electron, electron–phonon, and impurity/defect scattering.

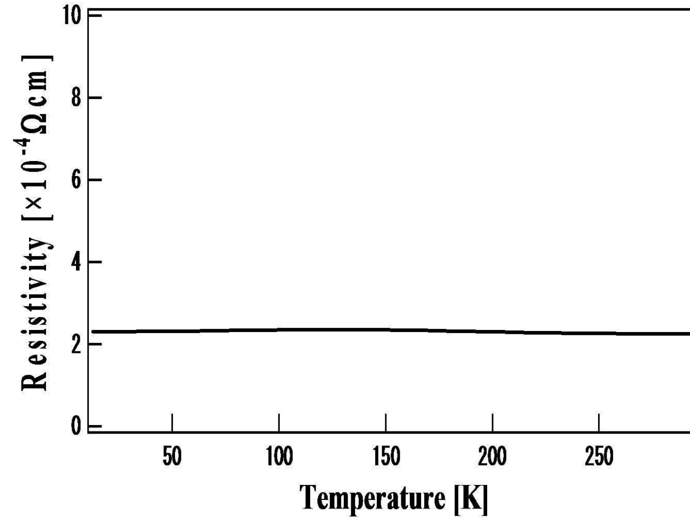

Figure 5. The resistivity-temperature curve of the LaB_6 thin film deposited on the ultrasmooth sapphire substrate.

CONCLUSIONS

C-axis (100) highly-oriented crystalline LaB_6 thin films could be fabricated on the ultrasmooth sapphire substrate with atomic steps of 0.2 nm in height and atomically flat terraces using a laser MBE. In the case of deposition on the commercial mirror-polished sapphire substrate, the grown film was amorphous. The (100) highly-oriented LaB_6 film exhibited a smooth surface with RMS roughness of 0.15 nm. The lattice parameter of the LaB_6 thin films was close to the bulk value reported previously. The growth behavior of LaB_6 nanocrystals has a possibility of in-plane crystal alignment or anisotropic crystallization concerning with the atomic steps. The resistivity of the prepared crystalline LaB_6 thin films was as low as 2.2×10^{-4} Ω cm and almost constant in the temperature range of 10–300 K.

ACKNOWLEDGMENTS

This work was supported in part by the Ministry of Education, Culture, Sports, Science and Technology of Japan, the National Institute of Advanced Industrial Science and Technology

of Japan, the New Energy and Industrial Technology Development Organization of Japan, and the Regional Innovation Creation R&D Program from the Ministry of Economy, Trade and Industry of Japan.

REFERENCES

1. D. Mandrus, B. C. Sales, and R. Jin, *Phys. Rev. B*, **64,** 012302 (2001).
2. M. Aono, R. Nishitani, C. Oshima, T. Tanaka, E. Bannai, and S. Kawai, *J. Appl. Phys.*, **50,** 4802 (1979).
3. M. Aono, C. Oshima, T. Tanaka, E. Bannai, and S. Kawai, *J. Appl. Phys.*, **49,** 2761 (1978).
4. C.-H. Chen, T. Aizawa, N. Iyi, A. Sato, and S. Otani, *Journal of Alloys and Compounds*, **366,** L6-L8 (2004).
5. M. Aono, T. Tanaka, E. Bannai, C. Oshima, and S. Kawai, *Phys. Rev. B*, **16,** 3489 (1977).
6. A. Hasegawa and A. Yanase, *J. Phys. F: Metal Phys.*, **7**, 1245 (1977).
7. T. Tanaka, T. Akahane, E. Bannai, S. Kawai, N. Tsuda, and Y. Ishizawa, *J. Phys. C: Solid State Phys.*, **9,** 1235 (1976).
8. H. Kawanowa, R. Souda, S. Otani, T. Ikeuchi, Y. Gotoh, P. Stracke, S. Krischok, and V. Kempter, *Surf. Sci.*, **482-485,** 250-253 (2001).
9. M. Zhang, L. Yuan, X. Wang, H. Fan, X. Wang, X. Wu, H. Wang, and Y. Qian, *J. Solid State Chem.*, **181,** 294-297 (2008).
10. R. J. Sobczak, and M. J. Sienko, *J. Less-Com. Metals*, **67,** 167 (1979).
11. Z. Fisk, H. R. Ott, V. Barzykin, and L. P. Gor'kov, *Physica B*, **312-313,** 808-810 (2002).
12. P. Vonlanthen *et al.*, *Physica B*, **284-288,** 1361-1362 (2000).
13. H. Zhang, Q. Zhang, J. Tang, and L.-C. Qin, *J. Am. Chem. Soc.*, **127,** 2862 (2005).
14. C. Mitterer, *J. Solid State Chem.*, **133,** 279-291 (1997).
15. T. Nakano, S. Baba, A. Kobayashi, A. Kinbara, T. Kajiwara, and K. Watanabe, *J. Vac. Sci. Technol. A*, **9,** 547 (1991).
16. I. Terasaki, S. Uchida, S. Tajima, K. Uchinokura, and S. Tanaka, *J. Phys. Soc. Jpn.*, **59,** 1017 (1990).
17. V. Craciun and D. Craciun, *Appl. Surf. Sci.*, **247,** 384-389 (2005).
18. D. J. Late, K. S. Date, M. A. More, P. Misra, B. N. Singh, L. M. Kukreja, C. V. Dharmadhikari, and D. S. Joag, *Nanotechnology*, **19,** 265605 (2008).
19. D. J. Late, M. A. More, P. Misra, B. N. Singh, L. M. Kukreja, and D. S. Joag, *Ultramicroscopy*, **107,** 825-832 (2007).
20. J. Tashiro, A. Sasaki, S. Akiba, S. Satoh, T. Watanabe, H. Funakubo, and M. Yoshimoto, *Thin Solid Films*, **415,** 272-275 (2002).
21. T. Maeda, M. Yoshimoto, T. Ohnishi, G. H. Lee, and H. Koinuma, *J. Cryst. Growth*, **177,** 95-101 (1997).
22. A. Sasaki, W. Hara, A. Matsuda, N. Tateda, S. Otaka, S. Akiba, K. Saito, T. Yodo, and M. Yoshimoto, *Appl. Phys. Lett.*, **86,** 231911 (2005).
23. W. Hara, J. Liu, A. Sasaki, S. Otaka, N. Tateda, K. Saito, and M. Yoshimoto, *Thin Solid Films*, **516,** 2889-2893 (2008).
24. A. Sasaki, J. Liu, W. Hara, S. Akiba, K. Saito, T. Yodo, and M. Yoshimoto, *J. Mater. Res.*, **19,** 2725 (2004).
25. M. Yoshimoto, T. Maeda, T. Ohnishi, O. Ishiyama, M. Shinohara, M. Kubo, R. Miura, A. Miyamoto, and H. Koinuma, *Appl. Phys. Lett.*, **67,** 2615 (1995).